THE AMERICAN SOCIETY OF MECHANICAL ENGINEERS
Three Park Avenue, New York, N.Y. 10016-5990

99-GT-33

FILM COOLING OVER A CONCAVE SURFACE THROUGH A ROW OF EXPANDED HOLES

Ping-Hei Chen*, Pei-Pei Ding*, Min-Sheng Hung* and Po-Chou Shih*
Department of Mechanical Engineering
National Taiwan University
Taipei 10617, Taiwan

ABSTRACT

This paper presents heat transfer coefficient and film cooling effectiveness measurements over a constant curvature concave surface. The coolant flow is ejected into the mainstream through a row of either simple holes or forward-expanded holes maintained at a streamwise injection angle (γ) of 35°. A transient liquid crystal thermography was employed to measure both the local heat transfer coefficient and film cooling effectiveness over the film-cooled concave test piece. With a pitch-to-diameter ratio (P/d) of 3, each forward-expanded injection hole has an expanded angle of 8° at the exit plane. In current study, the effect of blowing ratio (M) on film cooling performance was also investigated by varying the blowing ratio range from 0.5 to 1.5. Measurements were performed at mainstream Reynolds number (Re_d) of 2000 with turbulence intensity (Tu) of 2%, and coolant-to-mainstream density ratio (ρ_c/ρ_m) of 1.05. The curvature strength ($2r/d$) of test piece is 86.5. Comparisons were made with baseline cases of concave surface test piece with simple hole configuration done in prior studies. For forward-expanded hole configuration, measured results showed that both the laterally averaged heat transfer coefficient and film cooling effectiveness increase with increasing blowing ratio downstream of X/d = 10. A better film protection effect can be observed at M = 0.5 since coolant flows ejected at this blowing ratio might stay closer to the concave surface than other blowing ratios in present tested range for both hole configurations. As far as the hole shape is concerned, the forward-expanded hole injection provides better surface protection than the simple hole injection.

NOMENCLATURE

d	injection hole diameter on the inlet plane, [m]
h	heat transfer coefficient with film injection, [W/m²K]
h_o	baseline heat transfer coefficient without film injection, [W/m²K]
I	momentum flux ratio, = $\rho_c u_c^2 / \rho_m u_m^2$
L	length of injection hole, [m]
M	blowing ratio, = $\rho_c u_c / \rho_m u_m$
P	pitch of injection holes, [m]
q	heat flux per unit area, [W/ m²]
q_o	baseline heat flux per unit area without film injection, [W/ m²]
r	radius of curvature of concave surface, [m]
Re_d	mainstream Reynolds number based on the inlet diameter of injection hole,= $\rho_m u_m d / \mu$
t	time, [s]
T	temperature, [K]
Tu	mainstream turbulence intensity, [%]
u	velocity, [m/s]
X	axial distance from the center of injection hole, [m]
Y	spanwise coordinate from the center of injection hole, [m]
z	coordinate axis perpendicular to the test surface, [m]

Greek Symbols

α	thermal diffusivity of test surface, [m²/s]
δ_1	displacement thickness, [m]
ϕ	overall film cooling effectiveness, = $(T_w - T_m)/(T_c - T_m)$
γ	injection hole angle with respect to the test surface as projected into the streamwise/normal plane (inclination angle), [deg.]
η	film cooling effectiveness
$\overline{\eta}$	spanwise averaged film cooling effectiveness

* Professor
* Graduate Student

Presented at the International Gas Turbine & Aeroengine Congress & Exhibition
Indianapolis, Indiana — June 7–June 10, 1999

μ dynamic viscosity of mainstream, [kg/ms]
ρ density, [kg/ m^3]
τ time step, [s]

Subscripts

c coolant flow ejected from the injection hole
j index of the time step
m mainstream
s test piece
w surface of test piece
o initial condition
1 first test
2 second test

INTRODUCTION

For better engine efficiency, the quest for raising the combustor gas temperature into gas turbine becomes a challenge for researchers to develop a better cooling mechanism in protecting the gas turbine blade from the hot gas stream. Among these cooling mechanisms, film cooling has been widely used to protect the convex and concave surfaces of a turbine blade while the blade is exposed to an extremely hot inlet gas stream. For improvement of film cooling performance over these curved surfaces, research has been conducted extensively to obtain a better understanding of the film cooling characteristics.

A prior study about the film cooling performance over test pieces with different radius-of-curvature can be found by Ito and Goldstein (1971). Lately, Schwarz and Goldstein (1989) conducted both flow visualization and film cooling effectiveness measurements for film cooling over a constant radius-of-curvature concave surface through a row of simple holes. The film cooling effectiveness over the concave surface was obtained by measuring the impermeable wall concentration using a foreign tracer injection technique. They found that the mainstream instability over the concave surface enhances the mixing between the coolant flows and the mainstream. Consequently, the film cooling characteristics over the concave surface through a row of discrete circular holes are similar to those for a slot film cooling over a flat plate except for cases with low blowing rates and weak wall curvature. In the region near injection holes, reduction in film cooling effectiveness was observed with an increase in blowing ratio due to a greater penetration of the coolant flow into the mainstream. Schwarz et al. (1991) performed a study that investigated the film cooling performance over a constant radius-of-curvature convex surface. Over the convex surface, the experimental results of Schwarz et al. (1991) showed that the lift-off phenomenon of the coolant jets results in a decrease of film cooling effectiveness with an increase in blowing ratio. Goldstein and Stone (1997) discussed the effect of injection angle on the film cooling over both concave and convex surfaces. Their results showed that film cooling performance is less affected by injection angle of coolant flow at a low blowing rate of 0.5. However, more shallow injection angles provide better film cooling protection at moderate blowing rate of 1.0. Ko et al. (1986) also reported film cooling effectiveness results for both concave and convex surfaces through a single row of injection holes. However, the coolant holes in their work were located on a flat piece that was placed upstream of the curved test surfaces. Their measured results indicated that film cooling had wider coverage over the concave surface than that over the convex surface.

Based on the experimental results presented in prior studies, the film cooling performance will be reduced if lift-off of coolant flows from the protected surface occurs. Thus, an expanded hole was proposed by Goldstein et al. (1974) to replace the simple hole in order to keep the ejected coolant flow to stay close to the protected surface when coolant flow travels downstream. Consequently, a better film cooling performance was observed for the expanded hole than the simple hole. Similar conclusions were also drawn by Schmidt et al. (1996) for film cooling with compound angle injection through a row of expanded holes and by Chen et al. (1998) for the injection through a row of conical holes. It should be noted that the conical hole configuration is different from the forward-expanded hole configuration as described by Thole et al. (1996) and Wittig et al. (1996). For a conical hole configuration, the exit diameter of injection hole is maintained the same with the simple hole diameter, follows by a 8° even contraction from this fixed exit diameter down to the inlet of hole. Meanwhile, the forward-expanded hole configuration has fixed inlet diameter of injection hole, follows by a straight circular part maintained at this diameter, and finally an 8° expanded angle on leeward side of injection hole.

To the authors' knowledge, none of the published studies provides detailed heat transfer coefficient and film cooling effectiveness distributions over a curved surface with coolant injection through a row of expanded hole. The current work aims to obtain both local film cooling and heat transfer distributions on a constant radius curvature concave surface with coolant flow ejected through a row of forward-expanded holes. In the present study, the streamwise injection angle (γ) is 35° and the spanwise injection angle is 0°. For forward-expanded hole configuration, the expanded angle is fixed at 8°. A transient liquid crystal thermography (Ekkad et al., 1997a, b, and Chen et al. 1998) was employed to measure both film cooling effectiveness and heat transfer coefficient simultaneously. The effect of blowing ratio on the film cooling performance was investigated. For the present heat transfer measurements, the blowing ratio (M) was varied from 0.5 to 1.5 at a mainstream Reynolds number (Re_d) of 2000 with turbulence intensity of 2%, and the curvature strength ($2r/d$) of concave test piece is 86.5.

TRANSIENT LIQUID CYSTAL TECHNIQUE FOR THREE-TEMPERATURE SYSTEM

The present work employed a typical transient liquid crystal thermography as described by Yu and Chyu (1998). The test surface is suddenly exposed to a heated mainstream during a transient test. A one-dimensional semi-infinite solid assumption can be applied to obtain the local heat transfer coefficient (h) over the liquid crystal coated

surface without film injection. The one-dimensional transient heat conduction equation in z direction becomes:

$$k\frac{\partial^2 T}{\partial z^2} = \rho C p_s \frac{\partial T}{\partial t} \tag{1}$$

with initial condition:

$$t = 0 \qquad T = T_i \tag{2}$$

at boundary conditions:

$$z = 0 \qquad -k\frac{\partial T}{\partial z} = h(T_w - T_r) \tag{3}$$

$$z \rightarrow \infty \qquad T = T_i \tag{4}$$

where k, Cp_s, and ρ_s are the thermal conductivity, the specific heat, and the density of test piece, respectively. In addition, the convective heat transfer coefficient h is defined as

$$h = q/(T_w - T_r) \tag{5}$$

where q is the heat transfer per area from the gas stream to the surface, T_r is the local reference temperature. Typically, the local reference temperature is selected as the mainstream temperature.

The obtained dimensionless temperature at the convective surface ($z = 0$) is expressed as:

$$\frac{T_w - T_i}{T_r - T_i} = 1 - exp(\frac{h^2 \alpha t}{k^2}) erfc(\frac{h\sqrt{\alpha t}}{k}) \tag{6}$$

Heat Transfer Coefficient and Film Cooling Effectiveness

Film cooling over a surface is a three-temperature problem related to mainstream temperature (T_m), injection flow temperature (T_c), and wall temperature (T_w). The mixing of the mainstream flow and injection flow over the surface forms the reference temperature. That is, the reference temperature is not always a constant but depends on the level of interaction between the mainstream flow and the coolant flow. Attention to the condition that the wall heat flux is zero, T_r is equal to the wall temperature and is often termed as the adiabatic wall temperature T_{aw}. The magnitude of reference temperature now can be obtained by introducing a new parameter, film cooling effectiveness (η) defined as:

$$\eta = \frac{T_{aw} - T_m}{T_c - T_m}$$

or

$$T_r = T_{aw} = (1-\eta)T_m + \eta T_c \tag{7}$$

Substituting Eq.(7) into Eq.(6) to replace T_r, forms:

$$T_w - T_i = \left[1 - exp\left(\frac{h^2 \alpha t}{k^2}\right) erfc\left(\frac{h\sqrt{\alpha t}}{k}\right)\right] \times \left[\eta T_c + (1-\eta)T_m - T_i\right] \tag{8}$$

In order to evaluate the two unknowns, h and η, in Eq.(8), two film cooling measurement tests with different values of T_m and T_c have to be done. In the film cooling study, the application of transient liquid crystal thermography technique faces another problem about the raising of both the temperature of mainstream and coolant flow in step-change requirement. Therefore, the Duhamel's Superposition is applied to modified the time varying temperature rises at inlets of both mainstream and injection flow temperatures, and obtain the following expressions:

$$T_w - T_{i_1} = \sum_{j=1}^{N}\left[1 - exp\left(\frac{h^2\alpha(t_1 - \tau_j)}{k^2}\right) erfc\left(\frac{h\sqrt{\alpha(t_1 - \tau_j)}}{k}\right)\right] \times \left[\eta\, \Delta T_{c_1} + (1-\eta)\Delta T_{m_1} - T_{i_1}\right] \tag{9}$$

$$T_w - T_{i_2} = \sum_{j=1}^{N}\left[1 - exp\left(\frac{h^2\alpha(t_2 - \tau_j)}{k^2}\right) erfc\left(\frac{h\sqrt{\alpha(t_2 - \tau_j)}}{k}\right)\right] \times \left[\eta\, \Delta T_{c_2} + (1-\eta)\Delta T_{m_2} - T_{i_2}\right] \tag{10}$$

where subscripts 1 and 2 denote the first and second tests respectively, and ΔT_m and ΔT_c denote the step changes at the time instant τ_j of mainstream and coolant flow, respectively. Substituting measured wall temperatures at time t for two individual runs, both h and η values can be obtained by solving Eqs. (9) and (10) simultaneously.

Heat Flux Ratio

A better indicator to show the film cooling performance over a film-cooled test surface is the heat flux ratio with and without ejected coolant flow. This is due to the trend in the film cooling effectiveness and the heat transfer coefficient over the test pieces at the same location are not consistent with increasing blowing ratio (Mick and Mayle, 1988). Sen et al. (1994) introduced a new parameter called Net Heat Flux Reduction (NHFR) to specify the film cooling performance. The present adopted the expression for the heat flux ratio as defined by Ekkad et al. (1997b) and is given by

$$\frac{q}{q_o} = \frac{h(T_w - T_{aw})}{h_o(T_w - T_m)} = \frac{h}{h_o}(1 - \frac{\eta}{\varphi}) \tag{11}$$

where ϕ is the overall cooling effectiveness defined as $(T_w - T_m)/(T_c - T_m)$. For a typical gas turbine blade with film cooling, the overall cooling effectiveness can range from 0.5 to 0.8. In current study, ϕ = 0.6 is used.

EXPERIMENTAL APPARATUS AND PROCEDURES

The transient liquid crystal thermography was performed over test facility that consists of a wind tunnel, a curved test section, a coolant flow system, and an image processing system. Figure 1 shows the schematic view of the test facility. All film cooling measurements over the concave test pieces were performed in a suction type wind tunnel. Air mainstream is drawn by an axial blower and accelerated by a nozzle with an area contraction ratio of 9:1. The mainstream is then delivered through a honeycomb and enters into a set of stacked wire-screen heaters. The screen heaters produce a step temperature rise of the mainstream at the beginning of test. Downstream of the heater, the mainstream passes through a bar-grid turbulence promoter, the curved test section, a flow straightener, and then finally enters into the blower. In order to enhance the mainstream turbulence intensity, a biplanar bar-grid turbulence promoter (10 × 9 bars) with 3-mm-dia bars

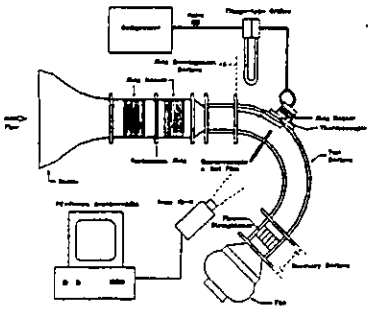

Figure 1 Schematic view of test facility.

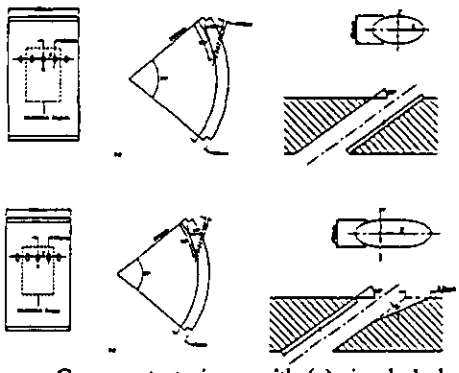

Figure 2 Concave test pieces with (a) simple hole configuration (b) 8° forward-expanded hole configuration.

was placed at 45.7 cm upstream of the injection holes.

The curved test section has a cross section area of 10 cm × 5 cm and a bend of 135°. Plexiglas was used for construction of test section and test pieces. The radii of curvature of the curved surfaces in the test section are 21.6 cm. In the present study, each concave test piece has either a row of simple hole or a row of forward-expanded injection hole. For convenience, the straight circular hole configuration is termed as the simple hole configuration in following text. For forward-expanded injection hole configuration, there are 5 forward-expanded holes on the row and each has an expanded angle of 8° on the exit plane follows by a straight circular inlet section. Figures 2 (a) and (b) show the geometrical dimensions of the concave test piece with simple and forward-expanded injection holes respectively. It is worth noting that the inlet hole diameter (d) of forward-expanded injection hole was smaller than the exit hole diameter ($\approx 1.5d$) since the forward-expanded injection hole had an expanded angle of 8° on the exit plane. For comparison, the same inlet hole diameter was used in the present study for both simple hole configuration and forward-expanded hole configuration. Thus, the concave test piece with simple hole configuration had less cut-off portion than that with forward-expanded hole configuration. For both hole configurations, the inlet hole diameter on the inlet plane, inclination angle, length-to-diameter ratio, and pitch-to-diameter ratio on the exit plane were d = 5 mm, γ = 35°, L/d = 3.5, P/d = 3, respectively. A spanwise injection angle of 0° was used.

Probes were inserted in instrumentation holes located at 1.5 cm upstream of injection holes for measurement of mainstream velocity, turbulence intensity, boundary layer displacement thickness and mainstream temperature. Three thermocouples of type T were placed at different spanwise locations with spacing of $3d$. Transient temperature response histories were recorded through a data logger (Gulton Rustrak, Rustrak-Ranger II), and a hot-film anemometer (Dantec, Flow Meter 54N60) measured the mainstream velocity. The turbulent intensity and displacement thickness of mainstream was respectively measured by TSI 1210-T1.5 and 1218-T1.5 hot-wire probes with the application of a TSI IFA-100 anemometer.

A compressor, a control valve, an orifice flow meter, a set of screen heaters, and a flow-settling chamber are used for the coolant flow loop. The coolant flow was supplied by a reciprocating-type compressor that has a capacity of producing an airflow rate of 0.0018 m^3/s at pressure of 7 atm. A calibrated flange-type orifice was used to measure the mass flow rate of coolant flow. In order to assure the uniformity of coolant flow ejected through the five injection holes, a porous plate was added in the settling chamber. In addition, a set of stacked wire-screen heater was also included in the settling chamber to heat up the coolant flow. A thermocouple of type T was placed in settling chamber for measurement of temperature response histories of coolant flow along heating.

The present image processing system includes a SONY Hi8 video camera, a Pentium II 266 MHz personal computer, a frame grabber, and a commercial image processing software LCIA V3.0 (Liquid Crystal Image Analyzer, Version 3.0). The Hi8 camera during each test run captured a complete recording of the color-changing image of liquid crystal. Color-changing images on tapes were then recorded by frame grabber and analyzed using the image processing software. In the current study, the time taken by coated liquid crystal to reach the threshold Green value was recorded at each measured pixel location, and used in the semi-infinite solid analysis to determine both heat transfer coefficient and film cooling effectiveness.

Each concave test piece for measurement was coated with a layer of liquid crystal (Hallcrest, BM/R38C5W/C17-10) in thickness of around several micrometers. To ensure the visibility and clarity of color change sequence in liquid crystal, a layer of black paint must be sprayed on the bottom of the transparent test piece. Before measurements, calibration for the color change temperature of liquid crystal is necessary. The in-suit calibration was conducted on a concave copper plate with T type thermocouples embedded at positions Y/d = -1, X/d = 2, 10, 20 within the measurement region. The calibration is started by the synchronized recording of transient temperature response histories by data logger and, color change image by video camera. The time taken value for liquid crystal to achieve the threshold Green value obtained from LCIA V3.0 software is matched with the transient temperature response histories by data logger. Therefore, the corresponding temperature of the threshold Green value will be obtained and this will be the calibrated temperature of the liquid crystal. The calibrated temperature of the liquid crystal in the present work was found to be 35.2°C for the desired threshold Green value. During calibration, the light source was installed at locations of 71 cm from the location X/d = 10 and was perpendicular to the concave surface.

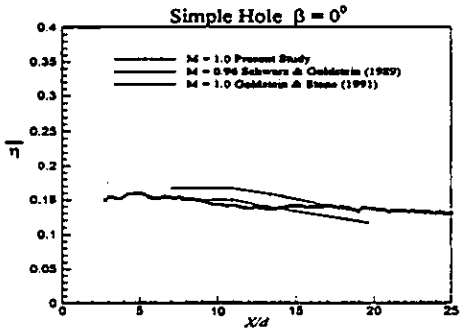

Figure 3 Comparison with prior measured results of spanwise averaged film cooling effectiveness over concave surface with simple hole configuration.

At the beginning of each film cooling measurement, the concave test piece was first assembled into the test section without changing the position of image capturing installation. After the coolant flow rate and the mainstream velocity were adjusted to the required values, both sets of screen heaters for mainstream and coolant flow were turned on simultaneously. Along with temperature rise in mainstream and coolant flow, the color of liquid crystal started to change. The data logger then recorded transient temperature response histories of the mainstream and coolant flow. Meanwhile, the color change history of liquid crystal on the concave test surface was recorded on the videotape. The image recorded by the videotape was replayed and analyzed by the software after the test was completed. As the times taken data of color change obtained from the image processing software and the temperature histories of mainstream and coolant flow recorded by the data logger were inputted into both Eqs. (9) and (10), the heat transfer coefficient and film cooling effectiveness at every measured pixel location can be determined. According to the current measurement experience, the time taken for color change of liquid crystal could vary from 20 sec to 200 sec, depending on the test conditions.

OPERATING CONDITIONS AND UNCERTAINTY ANALYSIS

The mainstream velocity (u_m) was kept at a constant value of 7.8 m/s in the current work but the velocity of coolant flow was varied to obtain the required blowing ratio. Based on the inlet diameter of injection hole, the mainstream Reynolds number is 2000. Measurements were conducted at four different blowing ratios of 0.5, 1.0, 1.25, and 1.5. The mainstream turbulence was promoted by an upstream bar-grid to a level of 2%. The density ratio (ρ_c/ρ_m) and the ratio of boundary layer displacement thickness to injection hole diameter (δ/d) were 1.05 and 0.162, respectively.

The uncertainty analysis with 95% confidence level on the measured parameters was conducted by the method proposed by Kline and McClintock (1953). The factors that result in the uncertainties of h and η are the mainstream temperature, coolant temperature, initial temperature, wall temperature and the time of color change as observed from Eqs. (9) and (10). Consequently, the total uncertainties of h (h = 23.9166 W/m^{2}K) and η (η = 0.1615) due to the five described factors

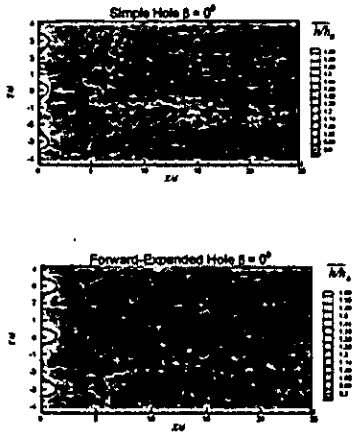

Figure 4 Local heat transfer coefficient ratio distributions at M = 1.5 for (a) simple hole configuration (b) 8° forward-expanded hole configuration.

were around 6.12% and 10.1%, respectively. Furthermore, the uncertainties for the Reynolds number, blowing ratio, mainstream turbulence intensity, boundary layer displacement thickness were 3.8%, 3.6%, 4.5%, and 5.3%, respectively.

RESULTS AND DISCUSSION

Baseline Experimental Results

A benchmark comparison was made with prior studies for the simple hole configuration over concave surface. Detailed test conditions were listed in Table 1. The comparison on spanwise averaged film cooling effectiveness ($\overline{\eta}$) of the three cases in Figure 3 showed similar trends along the streamwise direction. Schwarz and Goldstein (1989) stated that the change of relative strength of curvature ($2r/d$) may have an effect on spreading, but the small difference of $2r/d$ between Schwarz and Goldstein ($2r/d$ = 89) and the present test ($2r/d$ = 86.5) does not show any significant effect in this comparison.

Parameter / Authors	P/d	L/d	ρ_c/ρ_m	$2r/d$	γ	δ/d	M
Schwarz & Goldstein (1989)	3	10	0.95	89	35°	0.9	0.96
Goldstein & Stone (1997)	2.92	10	0.95	86.5	45°	1.19	1.0
The present study	3	3.5	1.05	86.5	35°	0.162	1.0

Table 1 Test conditions for the measured results shown in Figure 3.

Heat Transfer Results

Detailed distributions of local heat transfer coefficient ratio (h/h_o) for both simple hole and forward-expanded hole configurations are shown in Figure 4. Detailed distributions for only M = 1.5 are presented in this paper. Figures 5(a) and 5(b) illustrate the effect of blowing ratio on the spanwise averaged heat transfer ratio ($\overline{h/h_o}$) of both configurations for 2.8 < X/d < 25. The spanwise averaged results for regions X/d < 2.8 are not provided in this work since the one-dimensional heat conduction model used in data analysis might not be applicable to the three-dimensional thermal-fluid behavior around these injection holes.

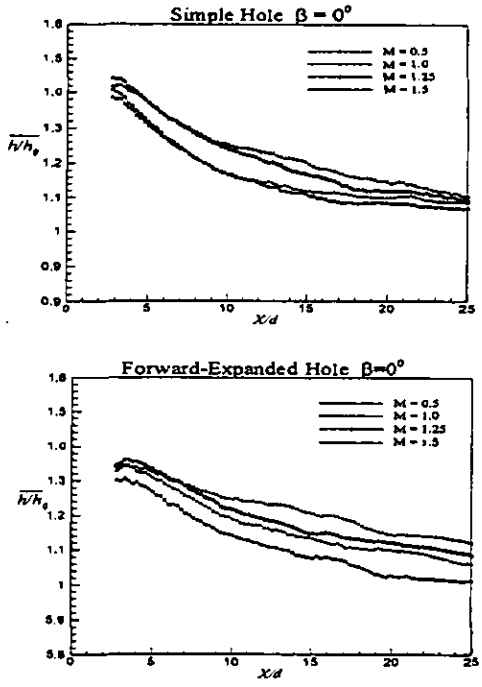

Figure 5 Effect of blowing ratio on the spanwise averaged heat transfer coefficient for (a) simple hole configuration (b) 8° forward-expanded hole configuration.

As indicated in Figure 4, the streamwise distributions of local heat transfer coefficient ratio trace the flow path of ejected coolant flow especially the forward-expanded hole configuration; whereas the spanwise distributions vary periodically with the spacing of discrete holes. When the coolant flow is ejected with higher blowing ratio (i.e. higher momentum ratio), its penetration into approaching mainstream causes high velocity gradient and hence separation may occur. This phenomenon significantly enhances heat transfer rate around both sides of injection holes. On the contrary, the lift off of ejected coolant flow produces a low heat transfer region just downstream the injection holes. This low heat transfer region is comparatively small and the magnitude of h/h_o is higher for the forward-expanded hole configuration as compared to simple hole configuration, shown in Figure 4(b). This evidence that the forward-expanded hole configuration can reduce the penetration of coolant flow into the mainstream boundary layer and perform better surface protection just after injection. Along streamwise direction, high heat transfer regions appear between two adjacent coolant jets. The single coolant jet structure constitutes of two counter-rotating vortex pairs is the cause. For $2.8 < X/d < 8$, the h/h_o distributions are similar in both configurations; nevertheless, enhanced heat transfer coefficients sustain far downstream for the forward-expanded hole configuration.

Downstream of X/d = 8, $(\overline{h/h_o})$ value increases with the blowing ratio in both hole configurations, as indicated in Figures 5(a) and 5(b). Regardless of change in blowing ratio, the magnitude of $(\overline{h/h_o})$ is relatively higher for simple hole configuration at all measured blowing ratios, an increase of 5% to 17% was documented. The lower magnitude of $(\overline{h/h_o})$ for forward-expanded hole configuration at all

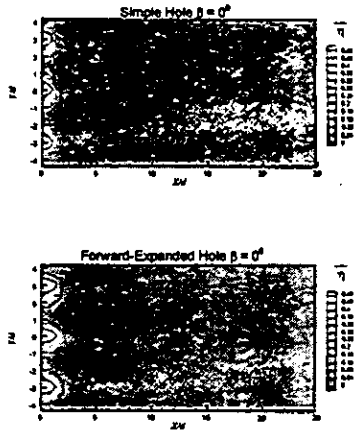

Figure 6 Local film cooling effectiveness distributions at M = 1.5 for (a) simple hole configuration (b) 8° forward-expanded hole configuration.

tested cases shows that the diffused hole can degrade the normal momentum of coolant jets effectively. For the simple hole configuration, the $(\overline{h/h_o})$ value declined along the streamwise direction at a given blowing ratio. For the tested blowing ratios in forward-expanded hole configurations, $(\overline{h/h_o})$ reaches a maximum around X/d = 4, and decreases smoothly downstream due to the momentum diffusion of coolant flow.

At $2.8 < X/d < 7$ for both configuration, as blowing ratio is increased to 1.5, lower $(\overline{h/h_o})$ is obtained as compared to M = 1.25. For simple hole configuration at M = 1.25, momentum flux ratio in the present study is I = 1.5 and $I\cos^2\alpha$ = 1.0. An increase of M to 1.5 leads to severe flow penetration at high tangential momentum flux of $I\cos^2\alpha$ = 1.5. Therefore, it contrarily causes less temperature gradient at the concave surface and a lower $(\overline{h/h_o})$ obtained. However, at X/d > 7, the return of jets to the wall results in an increased flow disturbance on surface, therefore the magnitude of $(\overline{h/h_o})$ grows up gradually. Goldstein and Stone (1997) observed similar phenomena from the flow visualization results. At a low blowing ratio of 0.5 (I = 0.24), the low $(\overline{h/h_o})$ is reasonable since coolant flow spread close to surface immediate after injection. That is, the interaction between the ejected coolant jets and mainstream is weakest among all tested blowing ratios.

The comparison of both hole configuration shows that forward-expanded hole configuration can perform better surface coverage since a decrease of 5% to 15% in $(\overline{h/h_o})$ can be obtained. The difference is especially obvious at low blowing ratio of M = 0.5.

Film Cooling Effectiveness Results

Figures 6(a) and 6(b) show the detailed distributions of local film cooling effectiveness (η) of both simple hole and forward-expanded hole configurations at M = 1.5. The passage of coolant flow obviously affects the distribution of η. High local film cooling effectiveness downstream of injection holes indicates that better film coverage exists. For simple hole injection, shown in Figure 6(a), an extremely low η region at hole edge follows by a moderately high η region around $2.8 < X/d < 5$, show the initial flow pattern of ejected

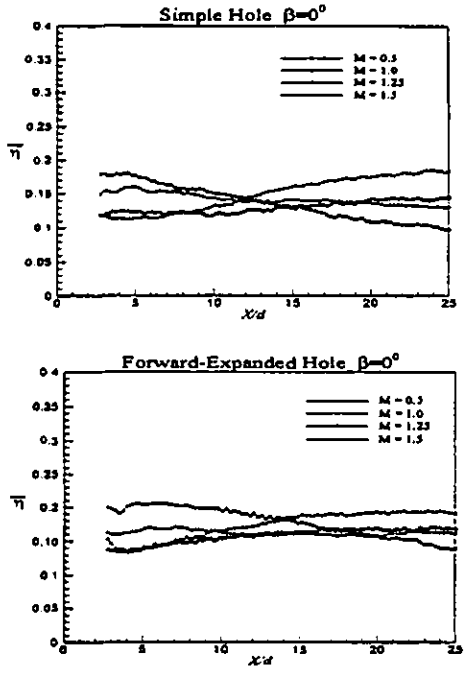

Figure 7 Effect of blowing ratio on the spanwise averaged film cooling effectiveness for (a) simple hole configuration (b) 8° forward-expanded hole configuration.

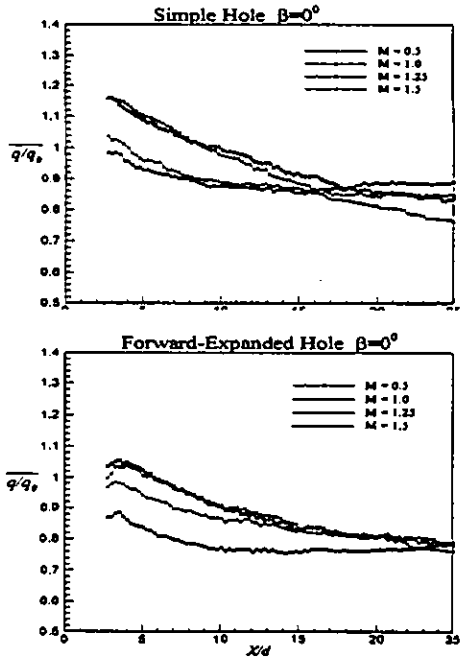

Figure 8 Effect of blowing ratio on the overall heat flux ratio for (a) simple hole configuration (b) 8° forward-expanded hole configuration.

coolant flow, which includes a lift-off, followed by a return of coolant flow to concave wall. However, regions between adjacent ejected coolant jets seem almost exposed to the mainstream with $\eta < 0.2$. This situation can be obviously relieved by using forward-expanded hole configuration. Figure 6(b) shows that under the same blowing ratio, the low effectiveness regions between adjacent ejected coolant jets become narrower and, the magnitude of η over $2.8 < X/d < 25$ is being increased from $0.16 < \eta < 0.36$ to $0.3 < \eta < 0.44$. Besides, the disappearance of the extreme low film cooling effectiveness region at downstream edge of hole in Figure 6(b) proved that a forward-expanded hole configuration is beneficial in suppressing the lift-off problem.

The results of spanwise averaged film cooling effectiveness ($\overline{\eta}$) at various blowing ratio for both hole configuration are shown in Figures 7(a) and 7(b). For $2.8 < X/d < 13$ of both configurations, the coolant flow with low normal momentum at blowing ratio of $M = 0.5$ spreads on the concave surface smoothly and protects it effectively. Moreover, the higher magnitude of $\overline{\eta}$ within this region for forward-expanded hole configuration indicates the better spanwise coverage of cooling film. At $X/d > 13$ for both configurations, an obvious increase in $\overline{\eta}$ for blowing ratio of $M \geq 1.25$, and a steep descent for $M = 0.5$ can be observed. This is reasonable because increased blowing ratio provides higher momentum and mass flow rate that yield higher effectiveness at downstream when coolant flows return to the concave wall. However, minimal penetration into mainstream and better surface coverage are yet needed for high film cooling performance. It is obvious that the diffused exit of forward-expanded hole can attain these insistences simultaneously at $M = 1.5$. Although injection through simple hole at $M = 1.5$ shows increasing $\overline{\eta}$ along streamwise direction too, but the local distribution of effectiveness (Figure 6(a) for $M = 1.5$) tells that high normal momentum promotes lift-off and cause poor coverage between adjacent coolant jets.

For the film cooling effectiveness, Schwarz et al. (1989) noted that the mass flux ratio has greater effects that momentum flux ratio at an injection angle near 45°. For the present study, coolant jets ejected through the 8° forward-expanded holes have a near 45° injection angle along the leeward side of holes. Therefore, an improved effectiveness is obtained at most downstream regions at higher blowing ratio. Comparison on both configurations shows that penetration of coolant flow into mainstream at higher blowing ratio can be effectively eased off by using forward-expanded hole configuration, an increase of greater than 20% in $\overline{\eta}$ is obtainable.

Heat Flux Ratio

The film cooling performance of test surface is best indicated by the results of spanwise averaged heat flux ratio shown in Figures 8(a) and 8(b). An obvious reduction in the heat flux ratio indicated that the film coverage effect of coolant flows performs better in forward-expanded hole configuration than the simple hole configuration for $0.5 \leq M \leq 1.5$. Downstream of $X/d = 10$, the distribution of q/q_o is no longer exhibited a descent trend, depending on the blowing ratio for both hole configuration. A plateau distribution for $M = 0.5$ is due to a faster momentum diffusion occurs. Generally, the magnitude of $\overline{q/q_o}$ lower than 1.0 at all tested blowing ratios for forward-expanded hole configuration indicates the better film cooling performance as compared to simple hole configuration.

It is interesting to note that $M = 0.5$ performs better over region $X/d \leq 13$ for both configurations. This phenomenon revealed the

coupled influence of high momentum and mass flow rate on the film cooling performance at higher blowing ratio. At $M = 0.5$, the low normal momentum of ejected coolant flow tends to depress the cooling jet onto the surface hence better performance obtained at $X/d \leq 13$, but the low mass flow rate slightly degrades its performance downstream. When M is increased to 1.25 and 1.5, the increased normal momentum promotes lift-off and therefore performs poor just after injection; the situation changes after coolant jets returned to the wall, the increased mass flow rate provides coverage further downstream and improves the performance.

CONCLUSIONS

The influences of hole configuration and blowing ratio on the heat transfer coefficient and film cooling effectiveness over a concave surface were investigated. The 8° forward-expanded hole configuration performs better spanwise coverage for all test cases with blowing ratios of 0.5, 1.0,1.25, and 1.5, especially at regions between adjacent coolant jets. Furthermore, best film protection effect can be observed at low blowing ratio of 0.5 among the present tested blowing ratios since coolant flows ejected at this blowing ratio might stay closer to the concave surface for both hole configurations.

For an inclination angle of 35°, measured results at various blowing ratios for the 8° forward-expanded hole configuration revealed that at higher blowing ratio, an improved film cooling performance over the whole measurement region can be obtained only if, the hole configuration can slightly decrease the normal momentum of ejected coolant jet. At higher blowing ratio, the increased mass flow rate of coolant flow causes increased effectiveness of both configurations at downstream region. The present study found that at high blowing ratio of 1.5, the 8° forward-expanded hole configuration can effectively reduce the lift-off phenomenon at $X/d \leq 10$, and provides better film coverage with the available mass flow at downstream region.

ACKNOWLEDGMENT

The authors deeply appreciate the financial support by NSC under the grant number 86-2212-E-002-080. The work in this study could not be achieved without their support.

REFERENCES

Chen, P. H., Ai, D., and Lee, S. H., 1998, "Effects of Compound Angle Injection on Flat-Plate Film Cooling through a Row Of Conical Holes" ASME Paper No. 98-GT-459.

Ekkad, S. V., Zapata, D., and Han, J. C., 1997a, "Heat Transfer Coefficients over a Flat Surface with Air and CO_2 Injection Through Compound Angle Holes Using a Transient Liquid Crystal Image Method," ASME *J. Turbomachinery*, Vol. 119, pp. 580-586.

Ekkad, S. V., Zapata, D., and Han, J. C., 1997b, "Film Effectiveness over a Flat Surface with Air and CO_2 Injection Through Compound Angle Holes Using a Transient Liquid Crystal Image Method", ASME *J. Turbomachinery*, Vol. 119, pp. 587-593.

Goldstein, R. J., Eckert, E. R. G., and Burggraf, F., 1974, "Effects of Hole Geometry and Density on Three-Dimensional Film Cooling," *Int. J. Heat Mass Transfer*, Vol. 17, pp. 595-607.

Goldstein, R. J., and Stone, L. D., 1997, "Row-of-Holes Film Cooling of Curved Walls at Low Injection Angles," ASME *J. of Turbomachinery*, Vol. 119, pp. 574-579.

Goldstein, R. J., and Yoshida, T., 1982, "The Influence of a Laminar Boundary Layer and Laminar Injection on Film Cooling Performance," ASME Paper No. 81-HT-38.

Kline, S.J. and McClintock, F.A., 1953, "Describing Uncertainties in Single-Sample Experiments," *Mechanical Engineering*, Vol. 75, pp. 3-8.

Ko, S.-Y., Yao, Y.-Q., Xis, B., Tsou, F.-K., 1986, "Discrete-Hole Film Cooling Characteristics over Concave and Convex Surfaces," *Heat Transfer 1986, Proceeding of 8th International Heat Transfer Conference, San Francisco*, Vol. 3, Hemisphere Publishing Corp., New York, pp. 1297-301.

Mick, W. J., and Mayle, R. E., 1988, "Stagnation Film Cooling and Heat Transfer, Including Its Effect Within the Hole Pattern," ASME *J. of Turbomachinery*, Vol. 110, pp. 66-72.

Schmidt, D. L., Sen, B., and Bogard, D. G., 1996, "Film Cooling with Compound Angle Holes: Adiabatic Effectiveness," ASME *J. of Turbomachinery*, Vol. 118, pp. 807-813.

Schwarz, S. G., and Goldstein, R J., 1989, "The Two-Dimensional Behavior for Film Cooling Jets on Concave Surfaces," ASME *J. of Turbomachinery*, Vol. 111, pp. 124-130.

Schwarz, S. G., Goldstein, R. J., and Eckert, E. R. G., 1991, "The Influence of Curvature on Film Cooling Performance," ASME *J. of Turbomachinery*, Vol. 113, pp. 472-478.

Sens, B, Schmidt, D. L., and Bogard, D.G., 1994, "Film Cooling With Compound Angle Hole: Heat Transfer," ASME Paper No. 94-GT-311.

Thole, K., Gritsch, M., Schulz, A., and Wittig, S., 1996, "Flowfield Measurements for Film-Cooling Holes with Expanded Exits," ASME Paper No. 96-GT-174.

Wittig, S., Schulz, A., Gritsch, M., and Thole, K. A., 1996, "Transonic Film-Cooling Investigations: Effects of Hole Shapes and Orientations," ASME Paper No. 96-GT-222.

Yu, Y., and Chyu, M. K., 1998, "Influence of Gap Leakage Downstream of Injection Holes on Film Cooling Performance," ASME *J. of Turbomachinery*, Vol. 120, pp. 541-548.